Bull. Mater. Sci., Vol. 38, No. 7, December 2015, pp. 1783–1790. © Indian Academy of Sciences.

Interaction of pristine hydrotalcite-like layered double hydroxides with CO_2: a thermogravimetric study

SHIVANNA MARAPPA and P VISHNU KAMATH*
Department of Chemistry, Central College, Bangalore University, Bangalore 560 001, India

MS received 19 May 2015; accepted 5 August 2015

Abstract. **Metal oxides in general have surface acidic sites, but for exceptional circumstances, are not expected to mineralize CO_2. Given their intrinsic basicity and an expandable interlayer gallery, the hydrotalcite-like layered double hydroxides (LDHs) are expected to be superior candidate materials for CO_2 mineralization. However, the incorporation of Al^{3+} adversely impacts the ability of the metal hydroxide layer to interact with CO_2 in the gas phase in comparison with the unitary $Mg(OH)_2$. Thermogravimetric analysis shows that the decomposition reaction of the [Mg–Al–CO_3] LDH is only marginally delayed in flowing CO_2 in comparison with flowing N_2, showing only an apparent marginal CO_2 uptake. Al^{3+} ion severely attenuates the surface basicity of the LDHs, as the unitary $Al(OH)_3$ is acidic in comparison with $Mg(OH)_2$ and shows little or no interaction with CO_2 in the gas phase.**

Keywords. **Layered double hydroxides; thermogravimetric studies; CO_2 uptake.**

1. Introduction

CO_2 is a greenhouse gas and the bulk of anthropogenic CO_2 production takes place at hydrocarbon-based power generating stations.[1] There is an urgent need to develop both the science and technology of CO_2 amelioration. One of the problems of CO_2 amelioration is the relative chemical inertness of CO_2 and its high thermodynamic stability. Three approaches are envisaged.[2] (i) Adsorption on a solid sorbent, (ii) dissolution in water and (iii) reaction with a solid.

Because of its chemical inertness, CO_2 physisorbs on most solid sorbents.[1] As is typical of physisorption, it is most efficient at low temperatures and high pressures. Competitive chemisorption of other gases (SO_x) if present along with CO_2 causes a rapid decline in the sticking coefficient of CO_2 on to the solid surface.[3] Flue gases typically have high content of N_2 and water vapour. In certain solids such as the zeolites, the presence of water vapour perilously decreases the probability of CO_2 sorption.[4]

Despite the significant solubility of CO_2, the quantity of water required to wash the flue gases is prohibitively large. The only option available is mineralization of CO_2 by a chemical reaction with a solid. A useful candidate solid for CO_2 mineralization applications should typically possess (i) high selectivity and uptake capacity for CO_2, and (ii) adequately rapid kinetics for reaction with CO_2.[5]

Among the solids explored to date, the layered double hydroxides (LDHs) have a high affinity for CO_2.[6] LDHs comprise ionocovalently bonded positively charged metal hydroxide layers having the composition $[M(II)_{1-x}M'(III)_x(OH)_2]^{x+}$ [M(II) = Ca, Mg, Co, Ni, Cu, Zn; M′(III) = Al, Cr, Fe; $0.2 \leq x \leq 0.33$]. The positive charge is compensated by inclusion of anions in the interlayer region. For convenience, the composition of the LDH is abbreviated by the symbol $[M–M'–A]_x$ (A = anion). Because of the high solubility of ambient CO_2 in water, dissolved CO_3^{2-} ions are ubiquitous in natural water bodies. Thereby LDHs crystallize by the inclusion of carbonate ions. In the laboratory, non-carbonate LDHs are synthesized by rigorous exclusion of CO_2 in the reaction medium. While the non-carbonate LDHs readily exchange anions[7] from the interlayer region for incoming carbonate ions, the carbonate–LDHs are inert to anion exchange reactions. Carbonates once incorporated cannot be exchanged except under acidic pH. The only way of expelling intercalated carbonate ions from the LDH crystal is by thermal decomposition. The intercalated CO_3^{2-} decomposes by the release of gaseous CO_2 and water in the temperature range 250–450°C in a reaction termed as deanation–dehydroxylation.

The gases evolved during thermal decomposition of LDHs have a character very close to that of the flue gases. The product of the decomposition reaction is an oxide. In some systems such as [Co–Al] LDH the decomposition temperature is adequate to form the thermodynamically stable spinel phase.[8,9] In others such as the [Mg–Al] system, the decomposition temperature (450°C) is much lower than the spinel formation temperature.[10] In such cases, the product is a defect oxide having the rocksalt structure, but with a significant trivalent cation content. This is not only structurally metastable, but is also nanoparticulate in morphology.[11] It rapidly reconstructs back into the original LDH structure either by taking dissolved carbonate ions from solution on soaking[12] or by taking up CO_2 from the ambient air on standing.[13] It is this property also called 'memory effect'[14]

*Author for correspondence (vishnukamath8@hotmail.com)

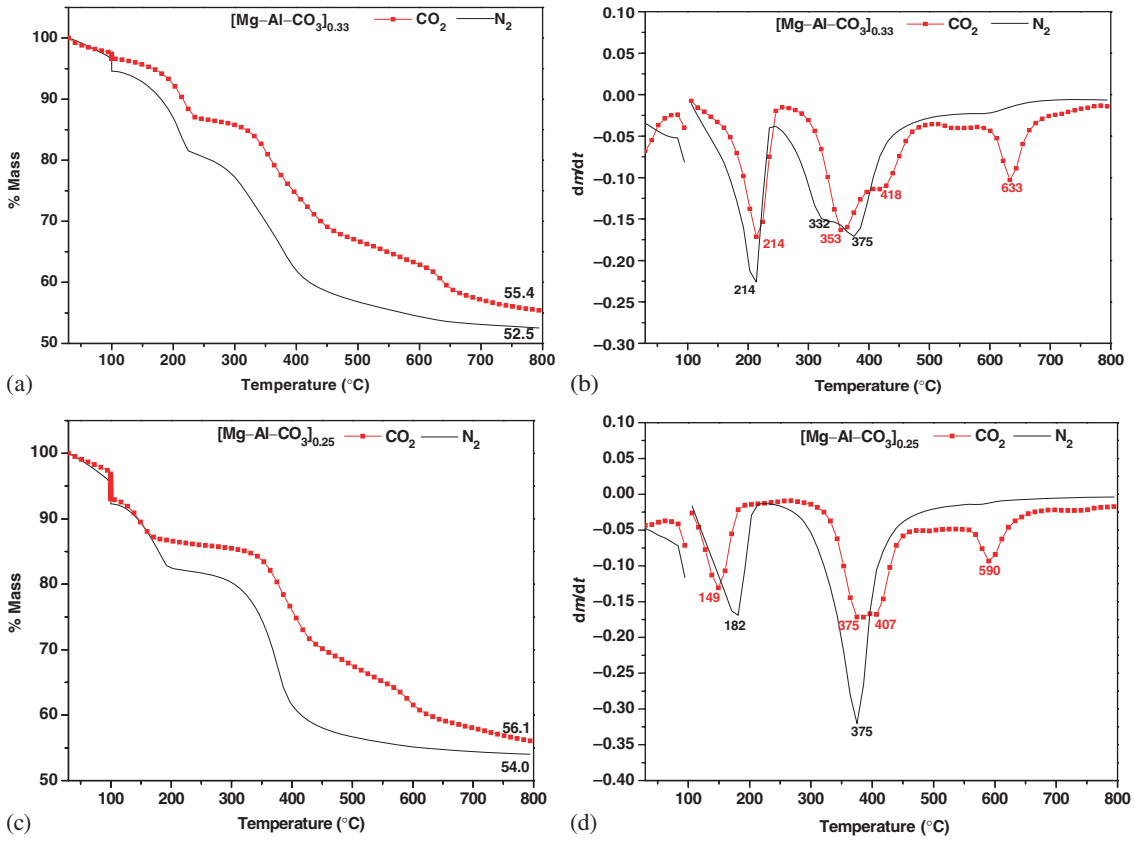

Figure 1. TGA profiles (**a**, **c**) and DTG curves (**b**, **d**) of [Mg–Al–CO_3] LDHs with $x = 0.33$ and 0.25, respectively. Dotted lines correspond to data obtained in flowing CO_2 and continuous line in flowing N_2.

Table 1. Temperatures at which the mass loss steps occur. Values in parentheses correspond to the mass loss in percentage.

		°C (% mass loss)					
	Composition	Step I		Step II		Step III	
System	(x)	N_2	CO_2	N_2	CO_2	N_2	CO_2
Mg–Al–CO_3^{2-}	0.33	100 (5.4)	100 (3.4)	214 (13)	214 (9.6)	332; 375 (34.1)	353; 418 (31.6)
	0.25	100 (7.7)	100 (7.0)	181 (9.9)	149 (5.8)	375 (28.4)	375; 407 (31.1)
	0.2	100 (8.1)	100 (10.0)	171 (7.9)	138.5 (3.5)	364 (29.1)	386; 418 (31.7)
Mg–Al–NO_3^-	0.33	100 (9.3)	100 (8.9)	—	—	439 (43.7)	472 (42.5)
	0.25	100 (14.5)	100 (12.2)	—	—	450 (40.9)	471 (40.6)
	0.2	100 (13.8)	100 (14.6)	—	—	429 (42.0)	451 (39.8)
	0.15	100 (13.5)	100 (15.0)	—	—	386 (38.4)	461 (40.0)
Mg–Al–EDTA	0.33	100 (11.9)	100 (11.4)	—	—	386 (49.5)	407 (47.7)
Mg–Al–PABA	0.33	100 (8.6)	100 (8.0)	—	—	375 (48.2)	396 (47.4)

that is thought to be useful in the application of LDHs as candidate materials for CO_2 mineralization.

Most CO_2 uptake studies on LDHs have been carried out on samples degassed at 150–200[15] or 200–400°C.[16–19] In the low temperature range, the LDHs are dehydrated and in the higher temperature range they are decomposed into their oxide residues variously referred to as mixed metal oxide (MMO)[20] or layered double oxide (LDO).[3] The CO_2 uptake capacity has been investigated as a function of composition, moisture content, the nature of the anion and heat treatment. It was found that intercalated CO_3^{2-} and low water content promotes CO_2 uptake. The best sorption capacity was reported to be 0.3 mmol g^{-1}.[15,19] In contrast, the presence of water in the feed gas was reported to enhance CO_2 uptake to twice this value.[3,18] The capacity was greatly enhanced to 15 mmol g^{-1} in alkali-promoted LDHs. But incorporation of up to 11 wt% K_2CO_3 makes such a material compositionally not comparable with the pristine LDHs.

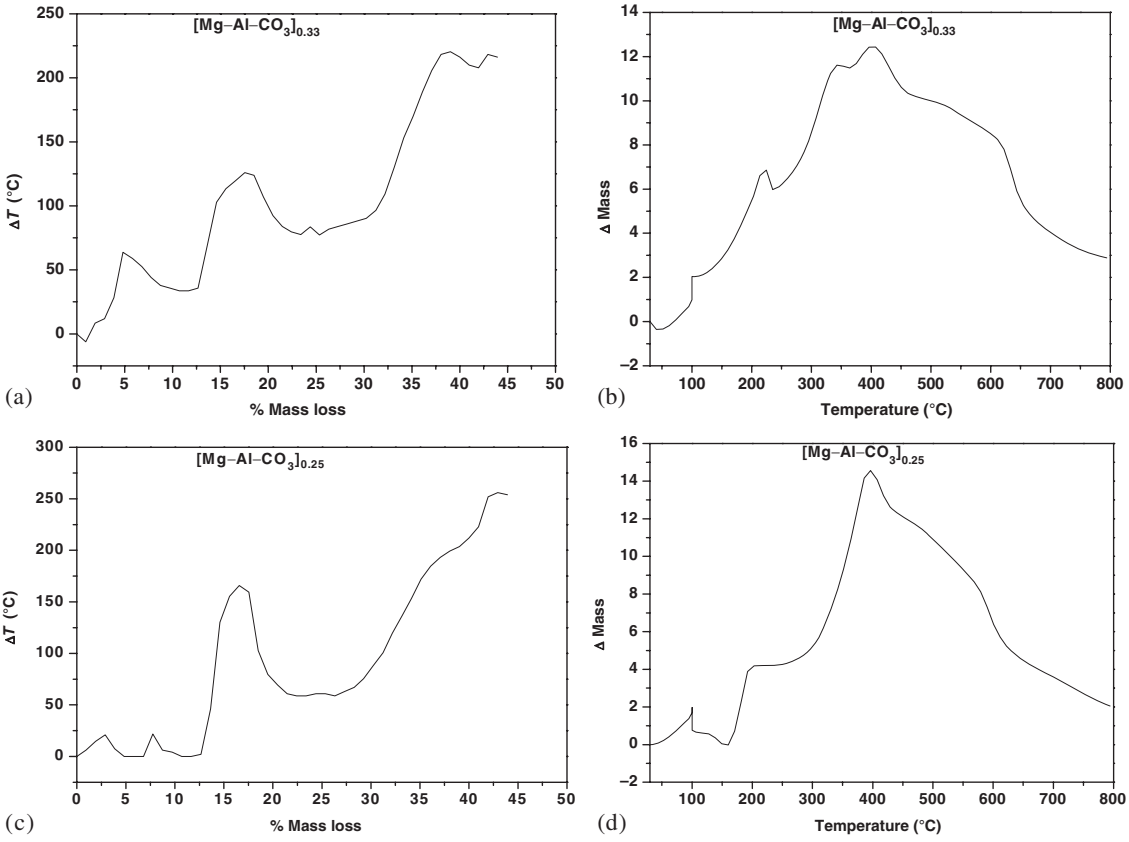

Figure 2. Plot of the difference in temperature (ΔT) at different mass loss values for [Mg–Al–CO_3] LDHs (**a**, **c**). A positive ΔT denotes a delayed mass loss in flowing CO_2. Plot of the differences in mass (Δm) at different temperatures (**b**, **d**) for [Mg–Al–CO_3] LDHs. Positive Δm denotes a lower mass loss in flowing CO_2.

The very first step in the exploration of any candidate material for CO_2 amelioration is to study its thermal behaviour in CO_2 atmosphere. In this paper, the thermal decomposition of a cohort of LDH samples is carried out in N_2 and CO_2. It is reported that the decomposition reaction takes place at a marginally higher temperature in flowing CO_2 than in flowing N_2, showing that the LDHs interact only weakly with CO_2 in the gas phase.

2. Experimental

2.1 *Synthesis of LDHs*

All chemicals used for synthesis were procured from the Merck (India) and used without further purification. Stock solutions of all metal salts were standardized before use. Deionized water (Type II, specific resistance 15 MΩ cm, Millipore Elix 3 water purification system) was used for the entire process. For the synthesis of non-carbonate LDHs, the deionized water was further decarbonated by boiling for 30 min and bubbling ultrahigh purity N_2 gas.

The [Mg–Al–CO_3]$_x$ LDHs were synthesized by coprecipitation by the method of Reichle.[21] In a typical synthesis, a mixed metal nitrate solution (50 ml, total metal concentration 1 mol l^{-1}) containing the required stoichiometric ratio of the divalent and trivalent metal ions ($x = 0.15$, 0.2, 0.25 and 0.33) was added to a beaker containing Na_2CO_3 and NaOH at high pH ∼12 slowly with constant stirring. The quantity of Na_2CO_3 taken was five times in excess of the stoichiometric requirement. The precipitate was aged at 65°C for 18 h before being centrifuged, washed, and dried at 65°C.

The [Mg–Al–NO_3]$_x$ LDHs were prepared by coprecipitation using ammonia. Ammonia precipitation not only helps to avoid carbonate contamination,[22] but also provides a constant pH ∼11 for the precipitation. In a typical coprecipitation, the mixed metal nitrate solution was added to a beaker containing ammonia (1 mol l^{-1}, 100 ml) with constant stirring within 10 min (dosing rate 5 ml min^{-1}). The reaction mixture was stirred for an hour and the slurry was aged in mother liquor (65°C, 12 h) before centrifugation.

The [Mg–Al–PABA]$_{0.33}$ LDH (PABA : *p*-aminobenzoic acid) was prepared by coprecipitation by the addition of a mixed metal nitrate solution to a vessel containing ten times the stoichiometric requirement of PABA taken in 100 ml water. A constant pH = 8 was maintained by simultaneously dispensing a NaOH solution (0.25 mol l^{-1}) using a Metrohm 718 STAT titrino operating in the pH stat mode. N_2 gas was

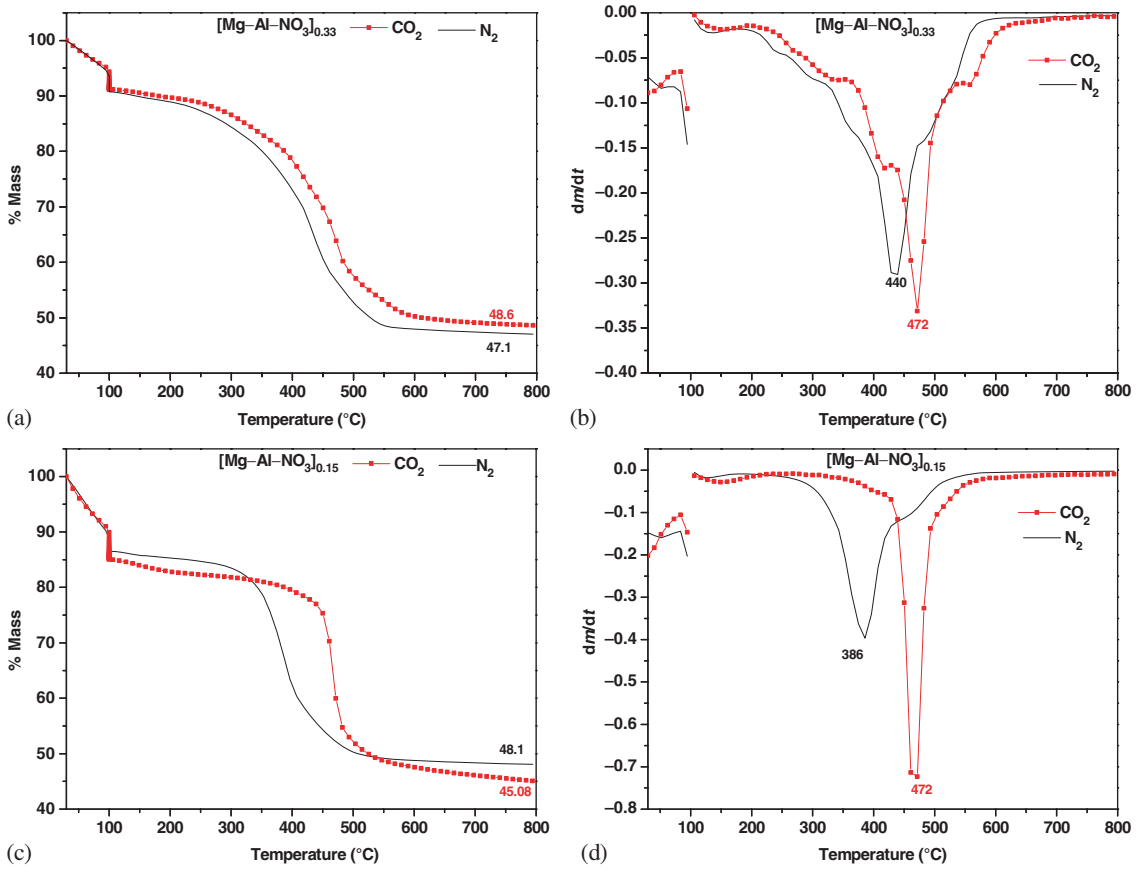

Figure 3. TGA profiles (**a**, **c**) and DTG curves (**b**, **d**) of [Mg–Al–NO_3] LDHs with $x = 0.33$ and 0.15, respectively. Dotted lines correspond to data obtained in flowing CO_2 and continuous line in flowing N_2.

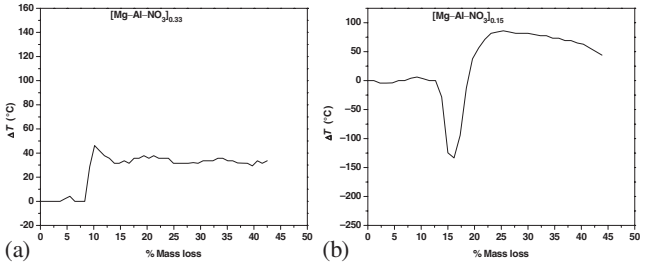

Figure 4. Plot of the difference in temperature (ΔT) at different mass loss values for [Mg–Al–NO_3] LDHs for (**a**) $x = 0.33$ and (**b**) $x = 0.15$. A negative value of ΔT denotes the early release of water in flowing CO_2.

purged during the reaction and the precipitation was carried out at 60°C. The precipitate was aged for 18 h.

The [Mg–Al–EDTA]$_{0.33}$ LDH (EDTA : ethylenediaminetetraacetic acid) was synthesized by anion exchange by suspending 0.5 g of the [Mg–Al–NO_3]$_{0.33}$ LDH in decarbonated water (20 ml) in a 100 ml screw capped bottle. A stoichiometric amount the disodium salt of EDTA was added to the bottle and kept for stirring overnight. All the products are washed thoroughly using decarbonated water, centrifuged, and dried in an oven at 60°C.

2.2 *Materials characterization*

All the products were characterized by powder X-ray diffraction (PXRD) using a Bruker D8 Advance diffractometer (source Cu Kα, $\lambda = 1.5418$ Å) operated in reflection geometry. The data were recorded at a continuous scan rate of 1° 2θ min^{-1}. Infrared spectra of all the samples were recorded using Bruker Model Alpha-P FTIR spectrometer (Diamond ATR cell, resolution 4 cm^{-1}, 400–4000 cm^{-1}). A detailed chemical characterization of this cohort of LDH samples is published elsewhere.[23] Thermogravimetric analysis (TGA) was carried out using a Mettler Toledo Model 851^e TG-SDTA system driven by Star^e software. A three segment heating program was employed comprising two ramps (30–100 and 100–800°C, heating rate 5°C min^{-1}, with a stay at 100°C for 1 h, flowing N_2 or CO_2, gas flow rate 50 ml min^{-1}).

3. Results and discussion

A comparison of the TGA data of the [Mg–Al–CO_3]$_x$ ($x =$ 0.33, 0.25 and 0.2) LDHs obtained in flowing N_2 and CO_2 (figure 1, table 1 and supplementary figure S1) shows that the mass loss steps are significantly delayed in flowing CO_2.

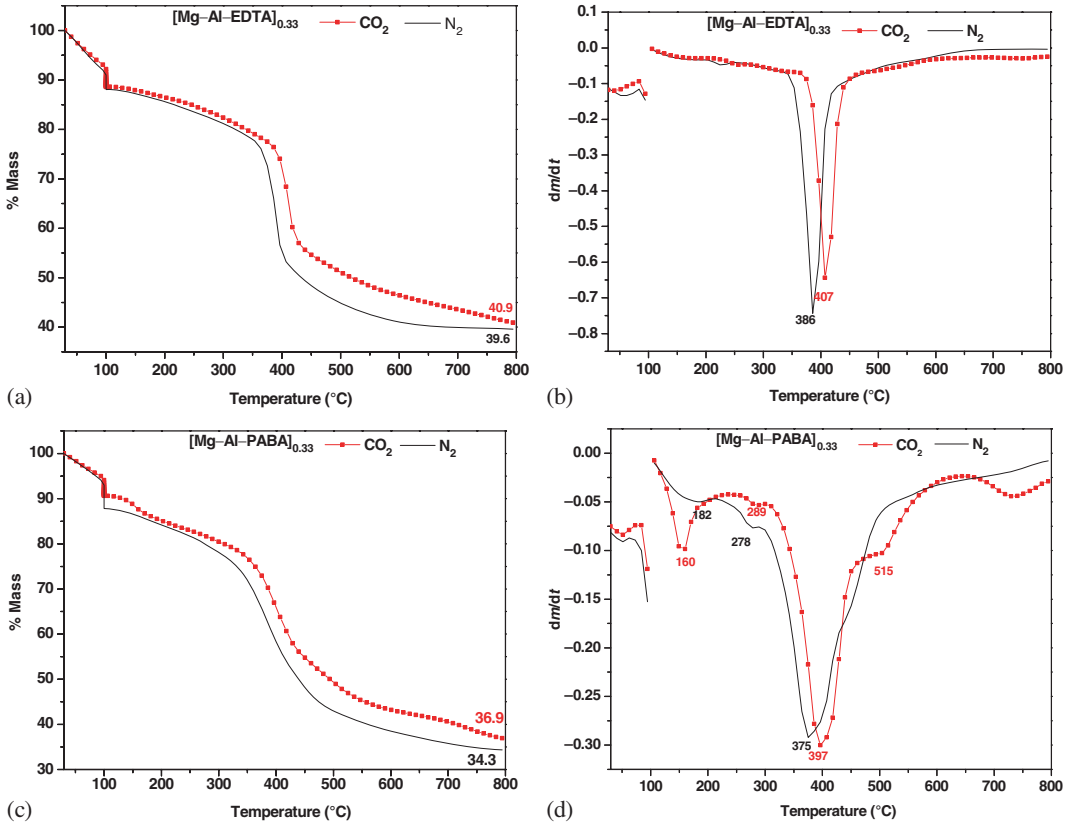

Figure 5. TGA profiles (**a**, **c**) and DTG curves (**b**, **d**) for [Mg–Al–EDTA] and [Mg–Al–PABA] LDHs, respectively.

The following observations are made.

(i) There is a significant mass loss on staying at 100°C (Step I), a process which shall be referred to as 'drying'. Under flowing N_2 the mass lost on drying increases from ∼5.4% ($x = 0.33$) to 8.1% ($x = 0.20$) when the layer charge decreases. Under flowing CO_2, this trend is preserved and the mass loss on drying increases from 3.4% ($x = 0.33$) to 10% ($x = 0.2$) (see table 1 and supplementary figure S1).

(ii) In the temperature range 100–800°C, there are two sigmoidal mass loss steps in flowing N_2, where as there are three steps in flowing CO_2.

(iii) In the case of $[Mg–Al–CO_3]_{0.33}$ LDH, the low temperature mass loss (Step II) occurs at the same temperature (214°C) in both the cases. However the extent of mass loss (13%) in flowing N_2 is higher than that (9.6%) in flowing CO_2. In LDHs of other compositions ($x = 0.25$ and 0.2), this loss occurs nearly 30°C earlier in flowing CO_2.

(iv) In the case of $[Mg–Al–CO_3]_{0.33}$ LDH, the high temperature (225–450°C) (Step III) loss is associated with two inflection points at 332 and 375°C in flowing N_2. In flowing CO_2 these are shifted to 353 and 418°C, respectively. LDHs of other compositions ($x = 0.25$ and 0.2) exhibit a single point of inflection in flowing N_2 and two points of inflection with delay in flowing CO_2.

(v) In flowing CO_2, an additional mass loss step is seen at 633°C (590°C in $x = 0.25$ and 0.20).

In summary, while the general behaviour of all CO_3^{2-}-LDHs is same, the LDH with $x = 0.33$ layer charge behaves in small details differently from other LDHs of lower layer charge.

A plot of ΔT (difference in the sample temperature in the two gases at a given mass loss) *vs.* % mass loss (figure 2a and c) exemplifies the range of mass loss in which the LDHs behave differently in the two gases. The temperature delay is maximum in the mass loss range 12–25 and 30–45% which correspond to the dehydration (Step II) and decomposition (Step III) steps, respectively. Further the quantity of mass loss in the dehydration step is lower in flowing CO_2 (table 1). The mass loss in the 100–800°C range is due to the following reactions:

$$\left[Mg_{1-x}Al_x(OH)_2\right](CO_3)_{x/2}\cdot yH_2O \rightarrow \left[Mg_{1-x}Al_x(OH)_2\right](CO_3)_{x/2} + yH_2O, \quad (1)\text{(Step II)}$$

$$\left[Mg_{1-x}Al_x(OH)_2\right](CO_3)_{x/2} \rightarrow (1-x)MgO + x/2Al_2O_3 + H_2O + CO_2. \quad (2)\text{(Step III)}$$

While the temperature delay of the decomposition step is expected based on Le Chatelier's principle, the suppression of the loss of intercalated water is surprising. The net effect is that flowing CO_2 appears to fix a certain proportion of

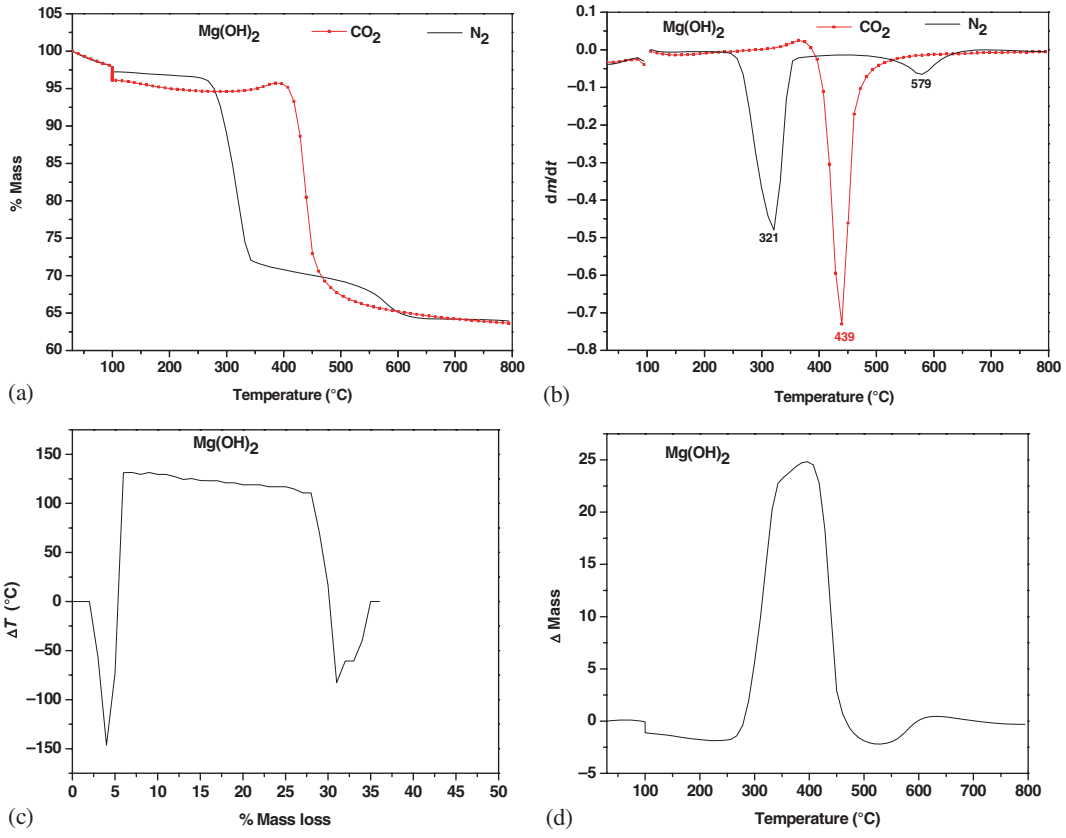

Figure 6. TGA profile (**a**), DTG curve (**b**), plot of the difference in temperature (ΔT) at different mass loss (**c**) and plot of the differences in mass (Δm) at different temperatures (**d**) for $[Mg(OH)_2]$. Dotted lines correspond to data obtained in flowing CO_2 and continuous line in flowing N_2.

intercalated water, while releasing the remaining at lower temperature than in flowing N_2. One reason for this behaviour could be the incorporation of ambient CO_2 as HCO_3^- ion by the reaction (i: intercalated; g: gas phase).

$$CO_3^{2-}\,(\text{i}) + CO_2\,(\text{g}) + H_2O\,(\text{i}) \rightarrow 2HCO_3^-\,(\text{i}) \qquad (3)$$

However if such as a reaction were to take place quantitatively as shown belowj

$$\left[Mg_{1-x}Al_x(OH)_2\right](CO_3)_{x/2}\cdot yH_2O + CO_2 \rightarrow \left[Mg_{1-x}Al_x(OH)_2\right](HCO_3)_x + zH_2O, \qquad (4)$$

there would indeed be a mass gain. Since there is a mass loss although reduced, in this temperature range, it is likely that the reaction (4) takes place partially. The delayed decomposition in flowing CO_2 is also expressible as an apparent mass gain (Δm) at different temperatures (figure 2b and d).

The effect of CO_2 on $[Mg–Al–NO_3]_x$ LDHs (figure 3) is dramatically different at $x = 0.15$ when compared with LDHs of $x \geq 0.20$. In this system the outgoing gas is NO_2 and the decomposition reaction is not in equilibrium with the ambient CO_2. Thereby no dramatic changes are expected. Further the NO_3^-–LDHs are known to undergo a broad single step mass loss[24] with no clear resolution of the dehydration and decomposition steps. In flowing CO_2 a slight delay in the mass loss by ~30°C is seen for all compositions $x \geq 0.20$ (figure 3b, table 1 and supplementary figure S2). However at $x = 0.15$, there is a massive apparent delay of ~80°C over the range of mass loss from 20 to 40% (figure 3).

As this is a nonequilibrium system, a change in the ambient gas is not expected to affect the thermal decomposition of NO_3^-–LDHs. In keeping with this expectation, NO_3^-–LDHs of all compositions ($x = 0.15$, 0.25 and 0.33) decompose at ~470°C in flowing CO_2. Under N_2, the LDHs with $x = 0.25$, 0.33 decompose at ~450°C, whereas the LDH with $x = 0.15$ decomposes at 385°C. In this case, the apparent delayed decomposition in CO_2 is actually due to the catalysis of NO_3^- volatilization in the N_2 atmosphere at this composition (figure 4).

These observations are counterintuitive. The structure of NO_3^-–LDHs differ at different layer charges. The NO_3^- ion is intercalated with its molecular plane inclined at an angle ~70° to the metal hydroxide layer, resulting in higher basal spacing of 8.8 Å, at $x = 0.33$.[23] As the layer charge decreases, the angle of inclination also decreases and at $x = 0.15$, the NO_3^- ion is intercalated with its molecular plane parallel to the metal hydroxide layer and leading to a reduced basal spacing of 8 Å. As the charge on the NO_3^- ion is half that of the CO_3^{2-} ion, a close packing of NO_3^- ions in the interlayer is achieved at half the layer charge of CO_3^{2-}

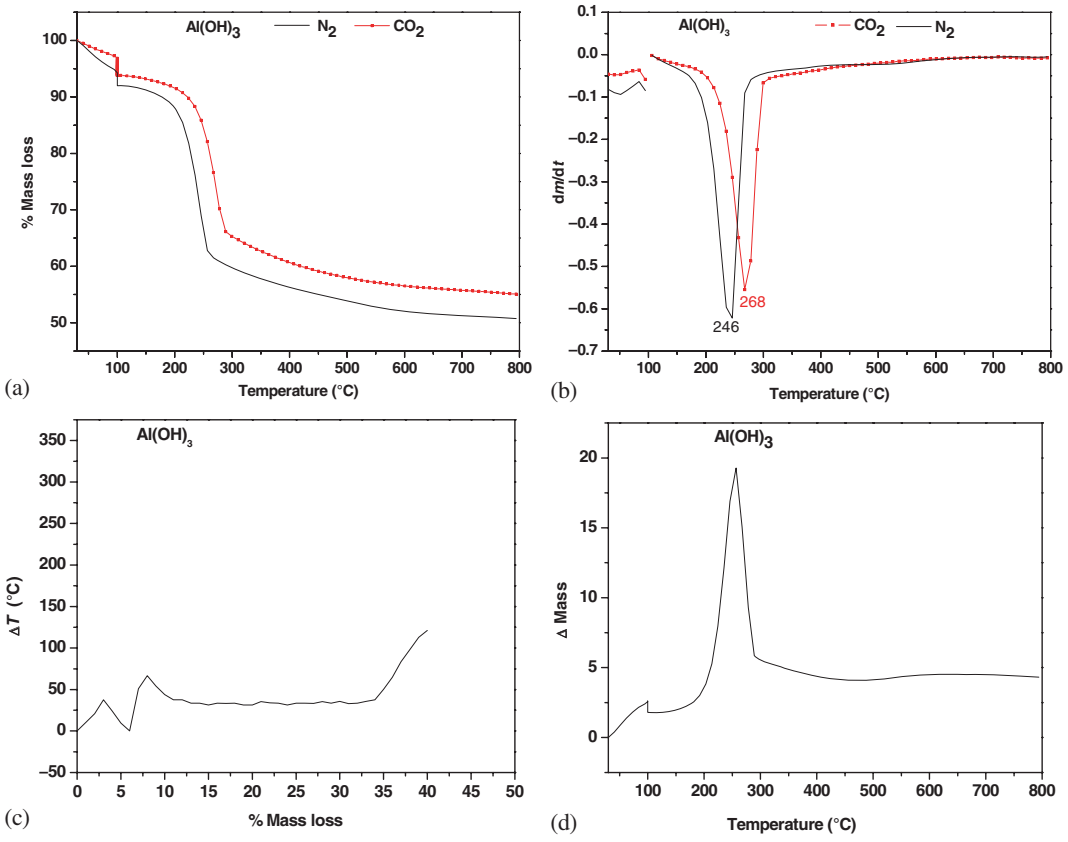

Figure 7. TGA profile (**a**), DTG curve (**b**), plot of the difference in temperature (ΔT) at different mass losses (**c**), plot of the differences in mass (Δm) at different temperatures and (**d**) for [$Al(OH)_3$]. Dotted lines correspond to data obtained in flowing CO_2 and continuous line in flowing N_2.

LDH. The volatilization of NO_3^- ions intercalated parallel to the metal hydroxide layer is catalysed in flowing N_2, but is unaffected in flowing CO_2. The temperature difference in the decomposition reaction can be expressed in the form of apparent mass gain (Δm) as a function of T (supplementary figure S3).

Amines are used as effective traps for CO_2. Therefore [Mg–Al–A] (A = EDTA and PABA) LDHs were prepared and decomposed in flowing N_2 and CO_2 (figure 5). In both cases, the decomposition was delayed in CO_2 nominally by 20–30°C. However no dramatic changes related to amine–CO_2 interaction could be observed. The observed temperature delay in the decomposition of non-carbonate LDHs under flowing CO_2 could be attributed to CO_2 molecules entering the interlayer space transiently, especially during the onset of decomposition.

There are numerous studies of CO_2 uptake by oxide residues obtained by the thermal decomposition of LDHs.[25–29] These oxide residues have a 3-D defect rocksalt structure and are erroneously referred to as LDOs. Oxides in general have surface acidic sites which are not conducive to CO_2 uptake. CO_2 is acidic and prefers basic sites. The LDHs with their intrinsic basicity should in principle be superior candidate materials for CO_2 uptake, in comparison with the oxides. It was this surmise that led to the present investigation of pristine LDHs. The totality of the results reported here show that the LDHs do not quite live up to these expectations. LDHs held at different temperatures in the entire range from the ambient till the decomposition temperature did not exhibit any mass gain, nor was there evidence of carbonate formation. Apart from the operation of Le Chatelier's principle operating in the case of CO_3^{2-}–LDHs, the temperature delay in mass loss was also nominal.

In order to understand these results better similar experiments were also carried out on the unitary hydroxides, $Mg(OH)_2$ (figure 6) and $Al(OH)_3$ (figure 7). In the case of $Mg(OH)_2$, the most dramatic results were observed with an ~118°C delay in decomposition in flowing CO_2, with apparent mass retention (Δm) over the temperature range 250–500°C. These effects are much less in the case of $Al(OH)_3$, with a marginal delay of ~21°C in the decomposition reaction. The difference in the behaviour of the unitary hydroxides is due to the differences in their basicity. $Al(OH)_3$ is more acidic than $Mg(OH)_2$. From a totality of results, it is evident that the incorporation of Al^{3+} drastically reduces the basicity of LDHs in comparison with the precursor $Mg(OH)_2$ and thereby deleteriously affects the efficacy of LDHs in acting as sinks for CO_2. Thereby alkali metal hydroxides and $Ca(OH)_2$ continue to remain as the best candidate materials for CO_2 amelioration.

4. Conclusions

The efficacy of a candidate material for CO_2 amelioration is critically dependent on the availability of surface and interlayer sites of high basicity. Pristine hydrotalcite-like LDHs despite their greater structural suitability for CO_2 amelioration are less effective than $Mg(OH)_2$ as Al^{3+} in the metal hydroxide layer reduces the basicity of the potential sites for CO_2 sorption.

Acknowledgements

We thank the Department of Science and Technology (DST), Government of India (GOI), for financial support. PVK is a recipient of the Ramanna Fellowship of the DST. We also thank the reviewer for some useful comments.

Electronic Supplementary Material

Supplementary material pertaining to this article is available on the Bulletin of Materials Science website (www.ias.ac.in/matersci).

References

1. Wang Q, Luo J, Zhong Z and Borgna A 2011 *Energy Environ. Sci.* **4** 42
2. Wang J, Huang L, Yang R, Zhang Z, Wu J, Gao Y, Wang Q, O'Hare D and Zhong Z 2014 *Energy Environ. Sci.* **7** 3478
3. Ram Reddy M K, Xu Z P, Lu G Q and Diniz Da Costa J C 2008 *Ind. Eng. Chem. Res.* **47** 7357
4. Jänchen J, Möhlmann D T F and Stach H 2007 *Stud. Surf. Sci. Catal.* **170** 2116
5. Yong Z, Mata V and Rodrigues A 2002 *Sep. Purif. Technol.* **26** 195
6. Williams G R and O'Hare D 2006 *J. Mater. Chem.* **16** 3065
7. Meyn M, Beneke K and Lagaly G 1990 *Inorg. Chem.* **29** 5201
8. Radha A V, Thomas G S, Kamath P V, Antonyraj C A and Kannan S 2010 *Bull. Mater. Sci.* **33** 319
9. Bellotto M, Rebours B, Clause O, Lynch J, Bazin D and Elkaim E 1996 *J. Phys. Chem.* **100** 8535
10. Valcheva-Traykova M L, Davidova N P and Weiss A H 1993 *J. Mater. Sci.* **28** 2157
11. Uzunova E L, Mitov I G and Klissurski D G 1997 *Bull. Chem. Soc. Jpn.* **70** 1985
12. Sato T, Kato K, Endo T and Shimada M 1986 *React. Solids* **2** 253
13. Rajamathi M, Nataraja G D, Ananthamurthy S and Kamath P V 2000 *J. Mater. Chem.* **10** 2754
14. Miyata S 1980 *Clays Clay Miner.* **28** 50
15. Yong Z and Rodrigues A E 2002 *Energy Convers. Manag.* **43** 1865
16. Ficicilar B and Dogu T 2006 *Catal. Today* **115** 274
17. Gao Y, Zhang Z, Wu J, Yi X, Zheng A, Umar A, O'Hare D and Wang Q 2013 *J. Mater. Chem. A* **1** 12782
18. Ram Reddy M K, Xu Z P, Lu G Q M and Costa J C D 2008 *Ind. Eng. Chem. Res.* **47** 2630
19. Radha S and Navrotsky A 2014 *J. Phys. Chem. C* **118** 29836
20. Zhao X, Zhang F, Xu S, Evans D G and Duan X 2010 *Chem. Mater.* **22** 3933
21. Reichle W 1986 *Solid State Ion.* **22** 135
22. Olanrewaju J, Newalkar B L, Mancino C and Komarneni S 2000 *Mater. Lett.* **45** 307
23. Marappa S, Radha S and Kamath P V 2013 *Eur. J. Inorg. Chem.* **2013** 2122
24. Kloprogge J T, Kristof J and Frost R L 2003 *2001—A Clay Odyssey* 451
25. Ram Reddy M K, Xu Z P, Lu G Q M and Costa J C D 2006 *Ind. Eng. Chem. Res.* **45** 7504
26. Wang Q, Gao Y, Luo J, Zhong Z, Borgna A, Guo Z and O'Hare D 2013 *RSC Adv.* **3** 3414
27. Chang P H, Chang Y P, Chen S Y, Yu C T and Chyou Y P 2011 *Chem. Sus. Chem.* **4** 1844
28. Beruto D T, Botter R, Lagazzo A and Finocchio E 2012 *J. Eur. Ceram. Soc.* **32** 307
29. Wang Q, Tay H H, Zhong Z, Luo J and Borgna A 2012 *Energy Environ. Sci.* **5** 7526